Brain (1997), **120,** 141–157

Localization of the motor hand area to a knob on the precentral gyrus
A new landmark

T. A. Yousry,[1] U. D. Schmid,[4] H. Alkadhi,[1] D. Schmidt,[2] A. Peraud,[3] A. Buettner[3] and P. Winkler[3]

Departments of [1]Neuroradiology, [2]Diagnostic Radiology and [3]Neurosurgery, Klinikum Grosshadern, Ludwig-Maximilian University, Munich, Germany and [4]Neurosurgical Unit, Klinik Im Park, Zurich, Switzerland

Correspondence to: Dr med. Tarek A. Yousry, Department of Neuroradiology, Klinikum Grosshadern, Marchioninistrasse, 15, D-81377 Munich, Germany

Summary
Using functional magnetic resonance imaging (fMRI) we have evaluated the anatomical location of the motor hand area. The segment of the precentral gyrus that most often contained motor hand function was a knob-like structure, that is shaped like an omega or epsilon in the axial plane and like a hook in the sagittal plane. On the cortical surface of cadaver specimens this precentral knob corresponded precisely to the characteristic 'middle knee' of the central sulcus that has been described by various anatomists in the last century. We were then able to show that this knob is a reliable landmark for identifying the precentral gyrus directly. We therefore conclude that neural elements involved in motor hand function are located in a characteristic 'precentral knob' which is a reliable landmark for identifying the precentral gyrus under normal and pathological conditions. It faces and forms the 'middle knee' of the central sulcus, is located just at the cross point between the precentral sulcus and the central sulcus, and is therefore also visible on the cortical surface.

Keywords: motor cortex; cortical anatomy; functional magnetic resonance imaging; palsy

Abbreviations: AVM = arteriovenous malformation; EPI = echo planar imaging; FLASH = fast low-angle shot; fMRI = functional magnetic resonance imaging; MPRAGE = magnetization prepared rapid acquisition gradient echo

Introduction
MRI allows the noninvasive study of the topography of the cortical surface with a high degree of spatial resolution. With the use of fast gradient-echo MRI sequences in subjects performing specific tasks, local changes in blood oxygenation and cerebral perfusion can be visualized that correlate in time with the onset and termination of the respective task. With this MRI technique, functional (fMRI) brain maps have been obtained of the human visual (Kwong *et al*., 1992; Connelly *et al*., 1993; Frahm *et al*., 1993; Menon *et al*., 1993; Ogawa *et al*., 1992; Turner *et al*., 1993) and motor (Kwong *et al*., 1992; Connelly *et al*., 1993; Constable *et al*., 1993; Kim *et al*., 1993*a*, *b*; Lai *et al*., 1993; Schad *et al*., 1993) cortices; these fMRI maps have been found to be compatible with the traditional teaching of functional representation. Comparison of the maps obtained through fMRI with those obtained during open brain surgery with full exposure and direct electrical stimulation of the sensorimotor strip (namely, the motor hand area) and of the adjacent cortex showed the maps to be almost identical, thereby validating fMRI (Puce *et al*., 1995; Yousry *et al*., 1995*b*).

Since the development of the concept of the 'homunculus' it has been known that the cortical representation of motor hand function is located in the superior part of the precentral gyrus (Foerster, 1936; Penfield and Boldrey, 1937; Penfield and Rasmussen, 1950). The 'homunculus' is usually projected onto the surface of an idealized precentral gyrus, where the representation areas are described in relation to each other, to the sylvian fissure, the median fissure and to the central sulcus rather than in reference to the intrinsic form of the pre- or postcentral gyrus. More recent studies using PET have shown that the sensory hand function is located in the central region at the superior genu of the central sulcus (Rumeau *et al*., 1994). However, PET did not allow for more

specific localization of this area, e.g. to the pre- or postcentral gyrus or to the anterior or to the posterior face of a specific gyrus.

Since the introduction of fMRI to localize motor hand functions, simple and complex paradigms have been used to detect areas responsible for motor hand control. Using fast low-angle shot (FLASH) gradient-echo sequences (Rao *et al*., 1993; Rao *et al*., 1995) as well as echo planar imaging (EPI) (Puce *et al*., 1995), simple movements—repetitive opening and closure of the hand (Yousry *et al*., 1995*b*), squeezing a sponge (Puce *et al*., 1995), tapping of all fingers in unison except for the thumb (Rao *et al*., 1993, 1995) or finger to thumb opposition (Jack *et al*., 1994), activated only the contralateral primary motor cortex. In contrast, more complex movements, sequential tapping of fingers in predetermined, fixed order (Rao *et al*., 1993) or repetitive opposition of the thumb and each of the remaining fingers (Kim *et al*., 1993*b*), could additionally activate the ipsilateral primary motor cortex, the supplementary motor area, the premotor and the somatosensory cortex bilaterally when using the FLASH (Kim *et al*., 1993*b*; Rao *et al*., 1993) or EPI (Atlas *et al*., 1996) technique.

When localizing a cortical structure or a lesion in the central region, it is essential to define the central sulcus or the precentral gyrus first. Several anatomical methods have been developed to identify the central sulcus using CT or MRI (Kido *et al*., 1980; Ebeling *et al*., 1989; Steinmetz *et al*., 1990; Rumeau *et al*., 1994; Naidich *et al*., 1995). But although the typical anatomy of the central region has been defined, identification of central region structures can still be difficult in some cases as reflected by the high variability of results obtained by different observers (Sobel *et al*., 1993), which in turn indicates the importance of additional landmarks or new imaging methods to locate these structures more reliably (Yousry *et al*., 1995*a*).

The study reported here had three objectives: (i) to localize and identify unique features on fMRI of the cortical area where motor hand function is represented; (ii) to describe the anatomical configuration of this area in detail in different planes, including possible variations using magnetization prepared rapid angle gradient echo (MPRAGE) sequences; (iii) to test the reliability of the new landmark for identifying the central region by having three readers evaluate MRI examinations independently, thus developing a new method to identify the precentral gyrus directly. The study was conducted in accordance with the Helsinki Declaration of 1983.

Subjects and methods

Localization of the motor hand area (step I)

MRI

In 10 healthy volunteers and in one patient, imaging was performed with a 1.5-T Magnetom (SP 63/Vision, Siemens, Erlangen, Germany). We used T_1- and T_2-weighted SE sequences and either a 3D FLASH sequence radio-frequency spoiled; flip angle = 20°, TR/TE = 15/6 ms, field of view = 200 mm, matrix = 256×256, spatial resolution, 0.8×0.8 mm^2/pixel), or a MPRAGE sequence (TR/TE = 12/4.4 ms, D = 500, TA = 13.38 min, AC (acquisition) = 1, field of view = 250×250 mm, matrix = 256×256).

fMRI

In 14 hemispheres of the healthy volunteers, a 2D FLASH sequence was used (Yousry *et al*., 1995*b*) with the following parameters: radio-frequency spoiled, TR/TE = 46.73/30.00 ms, field of view = 200 mm, matrix = 128×256, spatial resolution 0.8×1.6 mm^2/pixel (EPI was not available in our institution at the time of the study; it would have had some advantages such as higher temporal resolution, reduced motion artefacts and multi-slice acquistion; but these were countered to a certain degree by the lower spatial resolution related to the lower matrix of 64×64 and the higher field of view; we were only recently able to acquire images using the same matrix as in the setting presented here). A flip angle of 40° was used to allow visualization of flow effects and susceptibility related changes in sulcal veins (e.g. the central sulcal vein (Yousry *et al*., 1996)) and in venules of activated parenchyma (Jack *et al*., 1994; Yousry *et al*., 1995*b*) with one investigation. The parenchymal areas representing motor function of face (Jack *et al*., 1994), hand (Jack *et al*., 1994; Puce *et al*., 1995; Yousry *et al*., 1995*b*) and foot (Jack *et al*., 1994) defined using the FLASH (Jack *et al*., 1994; Puce *et al*., 1995; Yousry *et al*., 1995*b*) or EPI (Puce *et al*., 1995) technique have previously been validated using the 'gold standards' of either intrasurgical electrical stimulation mapping of the motor cortex (Puce *et al*., 1995; Yousry *et al*., 1995*b*), or perioperative sensory and motor stimulation mapping using subdural grids (Jack *et al*., 1994; Puce *et al*., 1995).

To examine the brain from the vertex to the corpus callosum, 9–13 sections were needed. Section orientation was axial and parallel to the bicommissural line. The specific task was a simple self-paced repetitive opening and closing of the hand at ~2/s. Twenty-seven measurements (each lasting 6 s) were obtained in each section: 11 before, six during, and 10 after, the motor task (Frahm *et al*., 1993).

fMRI data analysis

To detect areas of increased MR signal intensity that coincided with the motor task, images obtained before and during the task were summed for each section. The summed pre-task image was then subtracted from the summed task image for each section (Frahm *et al*., 1993). In these subtraction images, the relationship between signal intensity in all bright areas and time (time course of the inactive–active–inactive cycle) was determined by means of a software program that plotted the signal intensity for each of the 27 images of one cycle (Frahm *et al*., 1993; Kim *et al*., 1993*a*; Yousry *et al*., 1995*b*).

Only parenchymal areas in which the signal intensity changes corresponded to the time of task onset and completion were further analysed (Yousry *et al*., 1995*b*), the significance of these changes was assessed by means of the Mann–Whitney *U* test (Werner, 1984).

Correlation of anatomical and functional MRI results

The areas determined by fMRI to have a significant change in signal intensity were superimposed on that subject's anatomical MRI, and only areas that projected onto the parenchyma (Yousry *et al*., 1995*b*) and not onto the sulcus (Yousry *et al*., 1996) were taken into consideration. These activated areas were then superimposed on a single schematic (idealized) central region for of all examined subjects. The anatomical region where task-related activation of cortical structures was observed most frequently was measured and described. We have designated this anatomical structure simply as the 'motor hand area'.

Motion artefacts

To detect motion artefacts (i) consecutive images from each section were examined in cine mode to detect possible motion of the head, (ii) summed images were examined for blurred margins and (iii) subtracted images were examined for the presence of anatomical structures that would appear as a result of incongruencies in the summed images (Yousry *et al*., 1995*b*). Foam padding and vacuum cushions were used to immobilize the head within the coil. We did not judge motion artefacts to be severe enough in any subject to justify exclusion of the data from analysis.

Detailed anatomy of the typical motor hand area and variations (step II)

Anatomical dissection

Photographs and MRI (MPRAGE) were obtained of four formalin-fixed brain specimens before dissection. Then, the arachnoid membrane covering the surface was carefully removed to allow full exposure of the cortical surface. Subsequently, the surface of the central region was analysed to describe the relationship between the motor hand area in the depth of the central sulcus and its projection onto the surface. Next, seven brain hemispheres were dissected. Three hemispheres were dissected in the axial plane and four in the sagittal plane. On the eighth hemisphere, the postcentral gyrus was removed, and the base of the posterior face of the precentral gyrus was examined in detail.

MRI

MPRAGE sequences were obtained in 38 subjects (21 volunteers, 17 patients) and four anatomical brain specimens. Images were reconstructed with a slice thickness of 1 mm and a gap of 2 mm. The anatomical region defined previously as the motor hand area was assessed in all three anatomical planes. To define the precise location of the motor hand area, we identified the central sulcus and the precentral gyrus using the lateral axial (Kido *et al*., 1980) and the lateral sagittal (Naidich *et al*., 1995) methods, which were our 'gold standards' throughout this part of the study. Our analysis was simplified by the use of a (manufacturer supplied) software program that correlated the position of a certain point, marked on one plane, with its location on any other plane.

Details of typical motor hand area anatomy and variations

The shape of the motor hand area in patients and healthy subjects was analysed and measured in the axial and in the sagittal plane (59 hemispheres). This area was analysed similarly in slices of the anatomical specimens and in their corresponding MRI (seven hemispheres). From these data, we derived an anatomical definition of the motor hand area to guide identification of the precentral gyrus on axial and on sagittal slices in the next step of this study, establishing the significance of the motor hand area as a cortical landmark.

Clinical significance of the motor hand area as a cortical landmark (step III)

Anatomical features in patients

Anatomical features of the motor hand area were evaluated by MPRAGE sequences obtained in 41 hemispheres affected by a pathology in 29 patients.

Comparison of various methods for locating the precentral gyrus

One of us (T.A.Y.) used MPRAGE sequences to localize the precentral gyrus in 100 hemispheres of 50 subjects with three different techniques. The techniques located the gyrus by: (i) identifying the typical shape of the motor hand area, (ii) identifying the typical course of the superior frontal sulcus and the precentral sulcus (axial method; Kido *et al*., 1980), or (iii) following the course of the anterior horizontal and ascending branches of the sylvian fissure and the precentral sulcus (lateral sagittal method (Naidich *et al*., 1995)). The accuracy with which the gyrus could be identified using each technique was rated using an arbitrarily defined scoring system, in which '2' refers to 'identified with certainty', '1' to 'most probably identified' and '0' to 'not identified'. The point-to-point correlation feature of the software program we used ensured that the structure identified as the precentral gyrus was the same in the sagittal and in the axial plane.

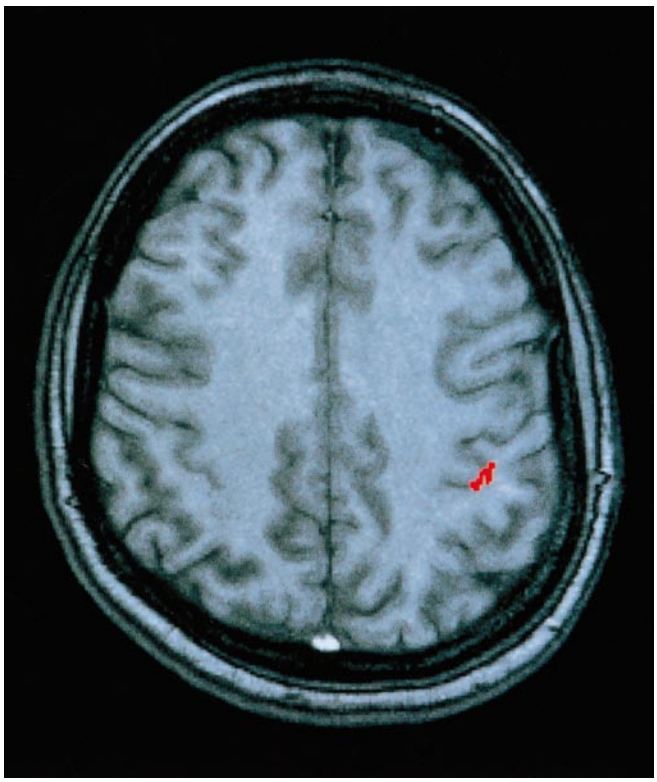

Fig. 1 An example of fMRI in a healthy volunteer showing an intraparenchymal area of activation (red) in the pre- (knob) and postcentral gyrus. Artefacts where the time courses of signal intensity changes and of the motor task did not coincide were excluded.

Interobserver variability in identifying the motor hand area

Three readers with various degrees of experience in analysing of brain MRI—a senior neuroradiologist (T.A.Y.), a senior neurosurgeon (U.D.S.) and a neurosurgeon in her second year of residency (A.P.)—independently evaluated the results of 100 MRI examinations using the three-point scoring system just defined. At that time in the course of this study, neither neurosurgeon had any experience in identifying the motor hand area on MRI, a measure taken to assess the ease with which the new method can be applied. When observers differed regarding the presence (score = 1 or 2) or absence (score = 0) of the motor hand area, a consensus was reached in a subsequent session, in which all three identification methods were used.

Results

Localization of the motor hand area

fMRI data analysis

In all healthy volunteers (14 hemispheres) a localized, significant ($P \leqslant 0.001$, U test) task-related increase in signal intensity (1.5–9.5%) was found (Figs 1 and 2), that projected into the brain parenchyma in the central region, contralateral to the task movement.

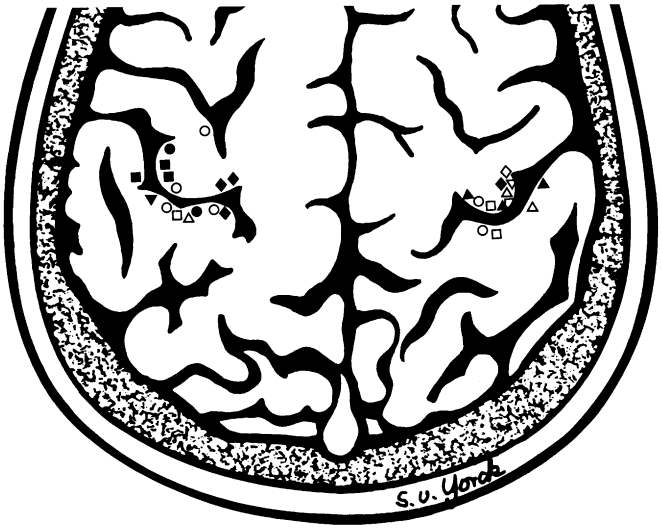

Fig. 2 Schematic drawing showing the location of the motor hand areas of activation as determined by fMRI in 14 hemispheres of 10 healthy volunteers. First, an exemplary axial drawing of an idealized omega shaped motor hand area was performed. Secondly, intraparenchymal areas of increased signal intensity found in each of the 14 examined hemispheres were transferred to a location corresponding to its original position (intrasulcal areas were disregarded), each symbol representing motor hand area(s) of one subject.

Correlation of anatomical and functional MRI results

These sites of signal intensity changes were located in the precentral gyrus in 11 hemispheres, in eight of the hemispheres additionally in the postcentral gyrus, and in three exclusively in the postcental gyrus (Fig. 2). Cortical sites on the precentral gyrus were consistently located on a broad based knob-like area of the posterior face ($n = 12$) (Figs 1 and 2). This knob had an inverted omega shape, was directed posterolaterally, and protruded into the central sulcus. One additional site of signal intensity change was found on the anterior face of the precentral gyrus in one right hemisphere. Sites of signal intensity change located on the postcentral gyrus were found directly opposite the knob on the anterior face of the postcentral gyrus (Figs 1 and 2).

Case report

A 68-year-old man (step I in Table 1) noticed a sudden loss of fine motor control and numbness of the tips of the fingers of his right hand. Neurological examination a few hours after this event revealed disturbed fine movements of the right hand and a moderate palsy (motor strength, M 4/5) of the muscles of the right hand. Sensory functions (algesia, stereognosia, pallaesthesia) in this hand were intact, except for a slight disturbance of positional sensibility of the fingers. Motor strength of the right arm was only minimally affected (M − 5/5). Neurological examination results in the contralateral upper limb and in the lower limbs were normal, cranial

Table 1A *Summary of subjects and techniques used to study the motor hand area*

Study step	Subjects (group*)	Brains (*n*)	Hemispheres (*n*)	Brains studied with each technique (*n*)			
				Functional MRI	Anatomical MRI		
				2D FLASH	3D FLASH	MPRAGE	SE sequence
I	Healthy (1)	10	14	10	10	–	10
	Patient (2)	1	1	–	–	1	1
II	Specimens (3)	4	7	–	–	4	–
	Healthy (4)	21	42	–	–	21	–
	Patients (5)	17	17	–	–	17	–
III	Patients (6)	50	100	–	3	–	47
	Healthy (4)	21	42	–	–	21	–
	Patients (5)	17	17	–	–	17	–
	Patients (7)	29	41	–	–	29	–

**See* details of groups of subjects in Table 1B.

Table 1B *Details of groups of subjects referred to in Table 1A*

Group	Details
(1)	Healthy subjects (women:men = 3:7; mean age 37.5 years; range 23–40 years, dominant:non-dominant = 7:7)
(2)	Patient (man, 68 years) with an ischaemic infarction in the 'precentral knob' of the left hemisphere (case report)
(3)	Specimens used for morphometric studies: cadavers without a history of endocranial pathology
(4)	Healthy subjects (women:men = 8:13; mean age 25 years; range 19–36 years)
(5)	Patients (women:men = 6:11; mean age 43.8 years; range 26–70 years): hemispheres not affected by a pathology
(6)	Patients (women:men = 26:24; mean age 52.5 years; range 23–87 years) randomly selected from routine neuroradiological examinations: only axial (n = 39); axial and sagittal (n = 10); only sagittal (n = 1); T_1 (n = 21), T_2 (n = 26), 3D FLASH (n = 3) Patients had unilateral tumours (n = 10; central region n = 3; temporal lobe n = 2; frontal lobe n = 2; parietal lobe n = 1; pituitary n = 1; ventricle n = 1), multiple sclerosis (n = 12), ischaemia (n = 12), aneurysms (n = 2), Parkinson's disease (n = 2), atrophy (n = 4)
(7)	Patients (women:men = 10:19; mean age = 44.5 years; range 9–70 years): tumours (n = 23; central region n = 9; temporal lobe n = 3; parietal lobe n = 2; ventricle n = 9), ischaemia (n = 2), cavernoma (n = 1), multiple sclerosis (n = 1), porencephaly (n = 1)

nerve function was undisturbed, and the results of clinical neuropsychological testing were normal.

On neurological examination two days later, fine movements and motor strength of this patient's right hand were still disturbed, but motor strength of the arm and sensory function had returned to normal. Duplex sonography of the cranial arteries gave normal results. Central motor conduction to the muscles of the arm and hand was assessed at this time with transcranial magneto-electrical stimulation of the head and neck and was found to be normal, as was central sensory conduction assessed with median nerve somatosensory evoked potentials.

Two days after the event, CT showed no abnormality in the brain, but MRI 4 days later showed a single distinct infarction (7 mm in diameter) that appeared hyperintense on the T_2- and proton-density-weighted sequences (Fig. 3) and hypointense on the T_1-weighted image. The infarction was located in the posterior face of the precentral gyrus, just posterior to the intersection of the superior frontal and precentral sulci, precisely within an epsilon-shaped protrusion into the central sulcus: the precentral knob (Fig. 3).

Detailed anatomy of the typical motor hand area and variations

Anatomical dissection

Superficially and starting from the midline, the course of the central sulcus in the eight cadaver hemispheres examined was sinusoidal and curved three times: the first curve (superior genu) was anteriorly convex, the second (middle genu) was posteriorly convex, and the third (inferior genu) was again anteriorly convex (Figs 4 and 5). After removal of the postcentral gyrus in one hemisphere, the posterior face of the precentral gyrus could be analysed along its full extent (Fig. 4). The middle genu had a smooth sinusoidal shape at the surface, but the curve became more pronounced (semicircular) in the depth of the sulcus. This was due to the presence of two small, anteriorly directed fissures, absent at the surface and increasing in depth towards the base of the central sulcus (Figs 4 and 5). These fissures were responsible for the inverted omega shape of the precentral gyrus on sections cut axially (Fig. 6) near its base, and for the hook shape of the gyrus when cut in the sagittal plane (Fig. 6).

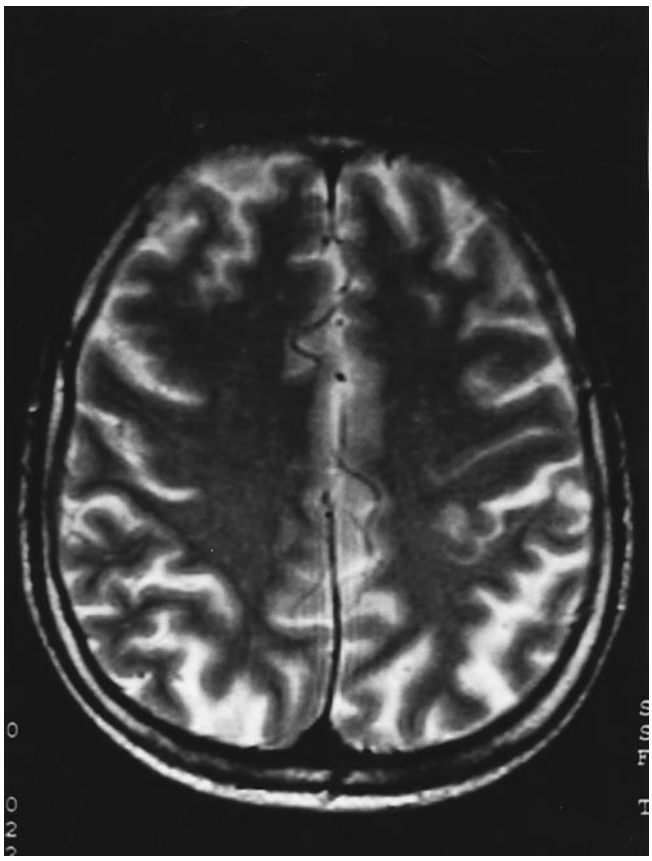

Fig. 3 T_2-weighted image in a 68-year-old man with sudden onset of an isolated palsy of the right hand. An isolated infarction can be detected in the epsilon-shaped knob of the left precentral gyrus.

The various distances measured on the anatomical dissection and the corresponding MRI are given in Table 2 (Fig. 7).

MRI

The knob-like structure was detected in all 59 hemispheres examined in the axial plane. It was of an inverted omega shape in 53 hemispheres (90%) and of a horizontal epsilon shape in six hemispheres (10%) (Figs 8 and 9). As found in specimens, the knob was always seated in the depth of the central sulcus at the apex of its posteriorly directed convexity (also designated the 'middle genu' (Figs 5, 6 and 8). The location of the knob was usually immediately posterior to the intersection of the superior frontal with the precentral sulcus. In the sagittal plane, the structure corresponding to the knob was hook-shaped (Figs 8 and 9) and was identified in 54 hemispheres (92%) (Table 3). In the remaining five hemispheres it could not be identified because of anatomical variations. The results of measuring the knob (Fig. 7) are listed in Table 2; the results are similar to those for anatomical specimens.

Definition

From the results just described we defined the motor hand area in the axial plane as a knob-like, broad based, posterolaterally directed structure of the precentral gyrus. It usually has an inverted omega shape and sometimes a horizontal epsilon shape with a mean diameter of 1.4 cm. On average it is located about 23 mm from the midline, just posterior to the junction of the superior frontal sulcus with the precentral sulcus and 19 mm from the lateral surface (Table 2). In the sagittal plane, this knob has the form of a posteriorly directed hook with a mean depth and height of 17 and 19 mm, respectively. It is located in the sagittal plane on the same section on which the insula can be identified, perpendicular to its posterior end.

Reliability of the precentral knob as a landmark

Anatomical features in patients

The dimensions of the knob in the sagittal and in the axial plane are given in Table 2. All measurements but one were within the ranges of the dimensions measured on unaffected hemispheres. The exception was the excessive height of the knob (D1) in one patient because of an arteriovenous malformation (AVM) that was located within the knob (Fig. 10).

Comparison of various methods to locate the precentral gyrus

The precentral gyrus was most frequently identified with certainty (score = 2) when the axial knob-detection method was used. The highest detection rates for the precentral gyrus in affected and unaffected hemispheres (score = 1 or 2) resulted from the axial knob, lateral axial and the lateral sagittal methods; the lowest rates arose from the sagittal knob (hook) detection method. Identification of the precentral gyrus on unaffected hemispheres was more reliable when the axial knob-detection or the lateral axial methods (mean score = 1.9) were compared with the sagittal knob-detection (hook) method (mean score = 1.7) (Table 4), and the differences were statistically significant.

Interrater variability in identifying the precentral knob

In the consensus discussion, the three readers agreed that, in the axial plane, the precentral knob (Table 4A) was present in 194 of 198 hemispheres (97.9%, Table 4) and was not present in four hemispheres. This structure was identified with a high degree of certainty by all three readers (score = 1.8–2.0). Failure to recognize the knob in the axial plane was due to the presence of a space-occupying lesion in three hemispheres and porencephaly in the fourth. In unaffected hemispheres, the sensitivity of the method was 97–100 %, with an accuracy of 97–100 %; in affected hemispheres, the sensitivity was 98–100 % with an accuracy of 98–100 % (Table 4A).

According to the consensus discussion, the precentral hook (Table 4B) was present in 113 of 122 hemispheres (92.6%)

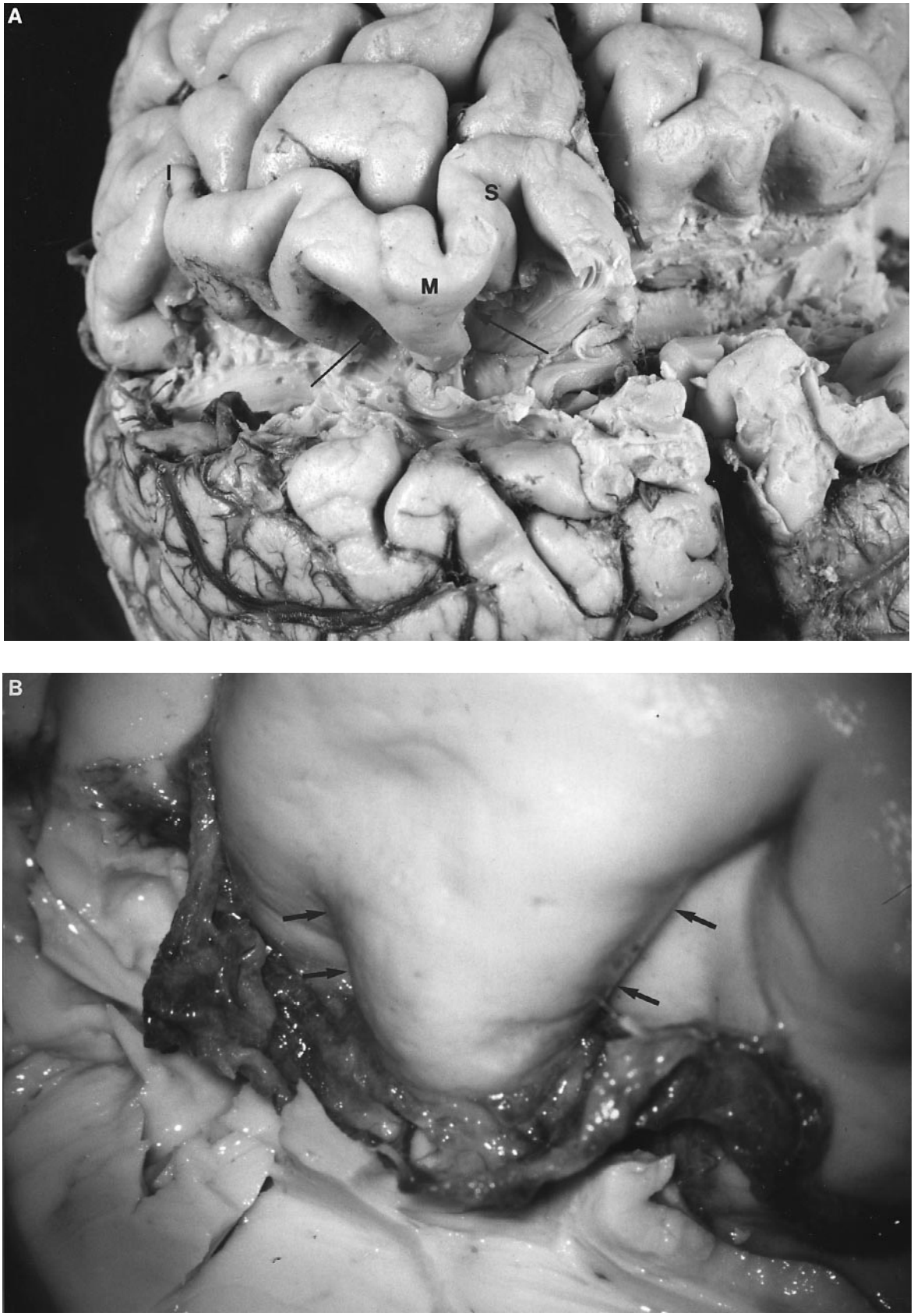

Fig. 4 Brain specimens after removal of the postcentral gyrus: the anteriorly directed superior genu (S), the posteriorly directed middle genu (M) and the anteriorly directed inferior genu (I) of the central sulcus (**A**). The slope of the curve of the middle genu has a sinus shape at the surface of the central sulcus. Two anteriorly directed fissures (arrows) are responsible for the semicircular or inverted omega shape of this genu that becomes more pronounced towards the base of the sulcus (**B**).

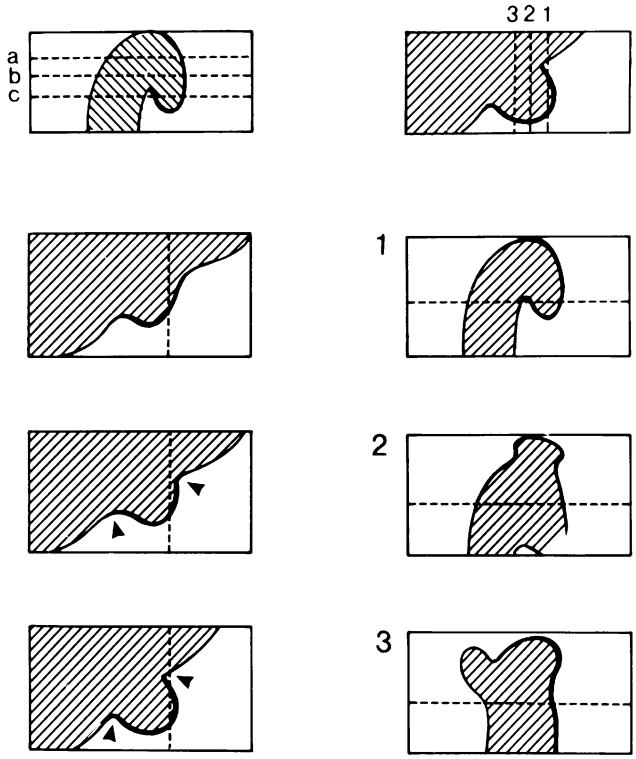

Fig. 5 Schematic drawing showing the change in shape of the middle genu of the left central sulcus from the surface (a) to the base (c) and from lateral (1) to medial (3). The smooth sinusoidal curve at the surface becomes omega- or epsilon-shaped towards the base of the central sulcus. In the axial plane (a–c), on the cortical surface, the posteriorly convex, middle genu of the central sulcus is composed of an apex, a medial and lateral smooth slope. In the depth of the central sulcus the apex remains unchanged, forming the knob. When the slopes change direction, bending inwards to form a semi-circle, then turning out again in a sharp angle, they give this knob its characteristic inverted omega shape (90.8% of hemispheres). The change of the slopes' curves from the surface to the base of the central sulcus is due to two anteriorly directed fissures, absent on the surface, reaching their farthest depth at the base of the sulcus, where they, short from meeting each other, lead to an 'insulization' or protrusion of a part of the precentral gyrus. Occasionally, a third fissure with a similar course between the latter two causes an additional segmentation of the knob, changing its appearance from an inverted omega to a horizontal epsilon (9.2% of hemispheres). In the sagittal plane (1–3), when cut precisely within the lateral fissure, this area has the form of a hook. It is the medially directed curved course of the lateral fissure that separates the posterior part of the precentral gyrus (e.g. knob) from its anterior part inferiorly, whereas they remain connected superiorly. The free appearance of the tip of the hook is a result of the decreasing volume of the knob towards the base of the sulcus. As a result, the hook can only be identified if the two fissures follow their described course and when the section passes through the lateral fissure (1).

and was not detected in nine hemispheres. The certainty of identification rated by the 3 readers was lower than for the axial method (score = 1.3–1.9). A space-occupying lesion and porencephaly prevented recognition of the hook in two out of nine hemispheres. In unaffected hemispheres, the sensitivity of this method was 86–100 % with an accuracy of 88–100 %; in affected hemispheres, the sensitivity was 97–100 % with an accuracy of 86–100 % (Table 4B).

Discussion

In this study, we could show that primary motor hand function is most frequently represented on the cortex in a specific segment of the precentral gyrus. Furthermore, this motor hand area has a characteristic shape: it is knob-like, most often having the form of an inverted omega (90%) or of a horizontal epsilon (10%) when examined in the axial plane, and it appears as a posteriorly directed hook (92%) when viewed in the sagittal plane. This finding was confirmed by the fact that in one patient a circumscribed ischaemic infarction in this knob was associated with selective motor palsy of the contralateral hand but not of of the arm, face or leg, and there was no sensory disturbance. This structure is so characteristic that it can easily and reliably be used to identify the precentral gyrus directly in healthy subjects and patients.

Anatomical location of the motor hand area

In a previous study using PET and MRI, Rumeau *et al.* (1994) showed that 'the superior genu of the central sulcus corresponds to hand function in the sensorimotor cortex'. They demonstrated a 'strict coincidence between the zone of increased blood flow' and 'the typical sigmoidal shape of the upper flexure of the central sulcus' in response to sensory (vibratory) stimulation of the contralateral palm of the hand (Rumeau *et al*., 1994). In the images shown in their report, they refer to an area that includes the knob we describe in this report.

In this study we used fMRI, which provides superior spatial resolution, and a motor stimulation model; we were therefore able to differentiate not only between activation of the precentral and the postcentral gyrus, but also between activation of the posterior or anterior face of these gyri. The accuracy of our model was confirmed by our findings in one case in which an infarction of this area caused an isolated palsy of that patient's contralateral hand. This corresponds to the classical lesion model.

As documented previously by us (Yousry *et al*., 1995*b*) and others (Kahn *et al*., 1996), we have detected areas of motor hand activation not only in the precentral gyrus, but additionally or exclusively in the anterior face of the postcentral gyrus. Three interpretations of this observation should be taken into account. First, mismatch between the anatomical and the functional images could allocate the activation from the central sulcus to the anterior face of the postcentral gyrus, e.g. from the central sulcal veins draining the activated hand area (Yousry *et al*., 1996). On the other hand, using fMRI (FLASH as well as EPI) it has been shown that activation can also be located to the walls of the central sulcus (Puce *et al*., 1995). This is in accordance with the observation of others (Allison *et al*., 1989)

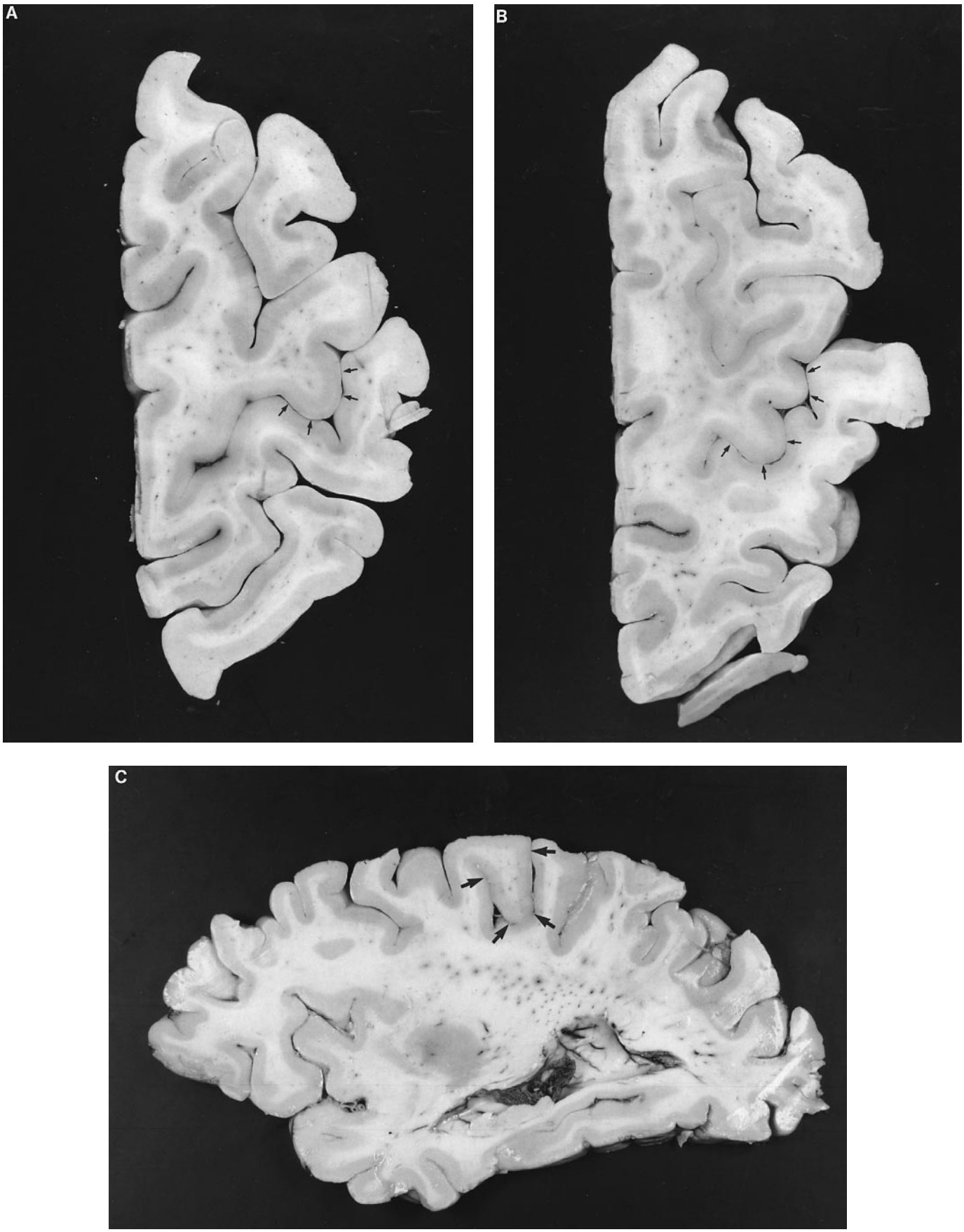

Fig. 6 Brain specimens showing the precentral knob, which can look like an inverted omega (**A**) or a horizontal epsilon (**B**) when cut axially, or like a posteriorly directed hook when cut sagittally (**C**).

Table 2A *Morphometry of the precentral knob (axial view, Ω, ε) in healthy subjects, in unaffected and affected hemispheres of patients, and in anatomical specimens*

	D1 (height in cm)				D2 (base in cm)				D3 (to midline in cm)				D4 (to lateral surface in cm)			
	Unaff	Aff	Specimens		Unaff	Aff	Specimens		Unaff	Aff	Specimens		Unaff	Aff	Specimens	
			MRI	Anat			MRI	Anat			MRI	Anat			MRI	Anat
n	59	39	3	3	59	39	3	3	59	39	3	3	59	39	3	3
Mean	0.8	0.9	0.8	0.7	1.4	1.4	1.6	1.5	2.3	2.5	2.2	2.2	1.9	2.0	1.8	1.8
SD	0.2	0.3	0.3	0.2	0.4	0.4	0.5	0.4	0.4	0.3	0.6	0.4	0.4	0.5	0.4	0.4
Min	0.4	0.5	0.4	0.5	0.8	0.7	1.1	1.1	0.9	1.8	1.7	1.8	0.9	0.6	1.5	1.5
Max	1.3	2.3	1.0	0.9	2.4	2.3	2.0	1.8	3.1	3.0	2.8	2.6	2.9	2.7	2.3	2.2

Unaff = unaffected hemispheres: both hemispheres of healthy subjects and non-affected hemispheres of patients [*see* (4) and (5) in Table 1B]; Aff = affected hemispheres of patients [*see* (7) in Table 1B]. MRI evaluation of hemispheres of dissected specimens [*see* (3) in Table 1B]; Anat = anatomical evaluation of hemispheres of dissected specimens [*see* (3) in Table 1B]; *n* = number of knobs measured: in the total of 107 hemispheres, the knob was not identified in two affected hemispheres (axial plane). *See* Fig. 7 for locations of dimensions D1–D4.

Table 2B *Morphometry of the precentral knob (hook, sagittal view) in healthy subjects, unaffected and affected hemispheres of patients, and in anatomical specimens*

	D5 (neck in cm)				D6 (base in cm)				D7 (height in cm)			
	Unaff	Aff	Specimens		Unaff	Aff	Specimens		Unaff	Aff	Specimens	
			MRI	Anat			MRI	Anat			MRI	Anat
n	54	39	4	4	54	39	4	4	54	39	4	4
Mean	1.0	1.1	1.0	1.1	1.7	1.9	1.9	2.0	1.9	1.9	2.0	2.2
SD	0.2	0.3	0.1	0.1	0.4	0.5	0.2	0.1	0.2	0.2	0.2	0.1
Min	0.6	0.3	0.9	1.0	0.9	0.5	1.6	1.9	1.4	1.1	1.8	2.1
Max	1.7	1.8	1.0	1.2	2.8	2.9	2.1	2.1	2.4	2.4	2.2	2.3

In the total of 107 hemispheres, the knob was not identified in two affected and five non-affected hemispheres (sagittal plane). *See* Fig. 7 for locations of dimensions D5–D7.

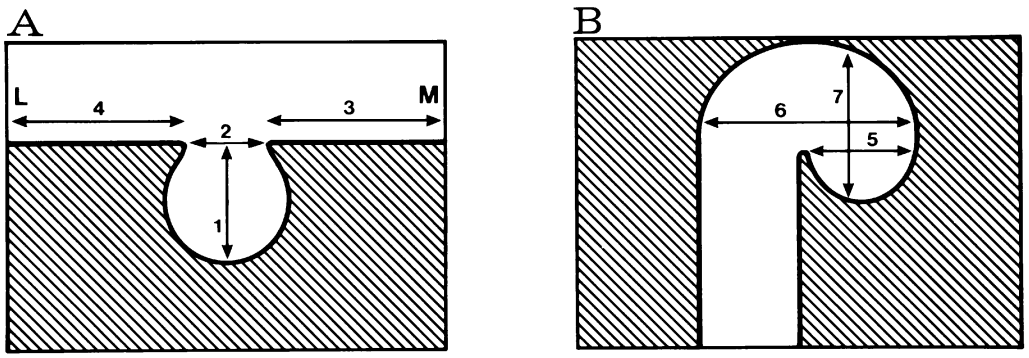

Fig. 7 Technique for measuring the knob in the axial (**A**) plane (L = lateral, M = medial) and in the sagittal plane (**B**). The numbers on the arrows indicate dimensions given in Table 2.

that sensorimotor function is not only represented in the crowns of the gyri visible at the cortical surface, but also in the walls of the central sulcus. Secondly, Foerster (1936), Penfield and Boldrey (1937) and Penfield and Rasmussen (1950) were able to elicit motor responses by stimulating the postcentral gyrus electrically. This overlap of sensory and motor function in the central area (Uematsu *et al*., 1992*b*) was documented later using fMRI (Puce *et al*., 1995; Yousry *et al*., 1995*b*; Kahn *et al*., 1996) or using subdural grid stimulation or recording (Uematsu *et al*., 1992*a*; Nii *et al*., 1996) in response to sensory or motor paradigms. This is in line with cytoarchitectonic evidence that pyramidal cells can be found in the pre- as well as in the postcentral gyrus (Brodmann, 1909). The postcentral gyrus thus contributes to the formation of the pyramidal tract and may therefore be additionally activated by the efferent part of the motor task. Thirdly, sensory (proprioceptive as well as exteroceptive) afferents can be activated by positional changes of the hand and fingers during performance of the motor task,

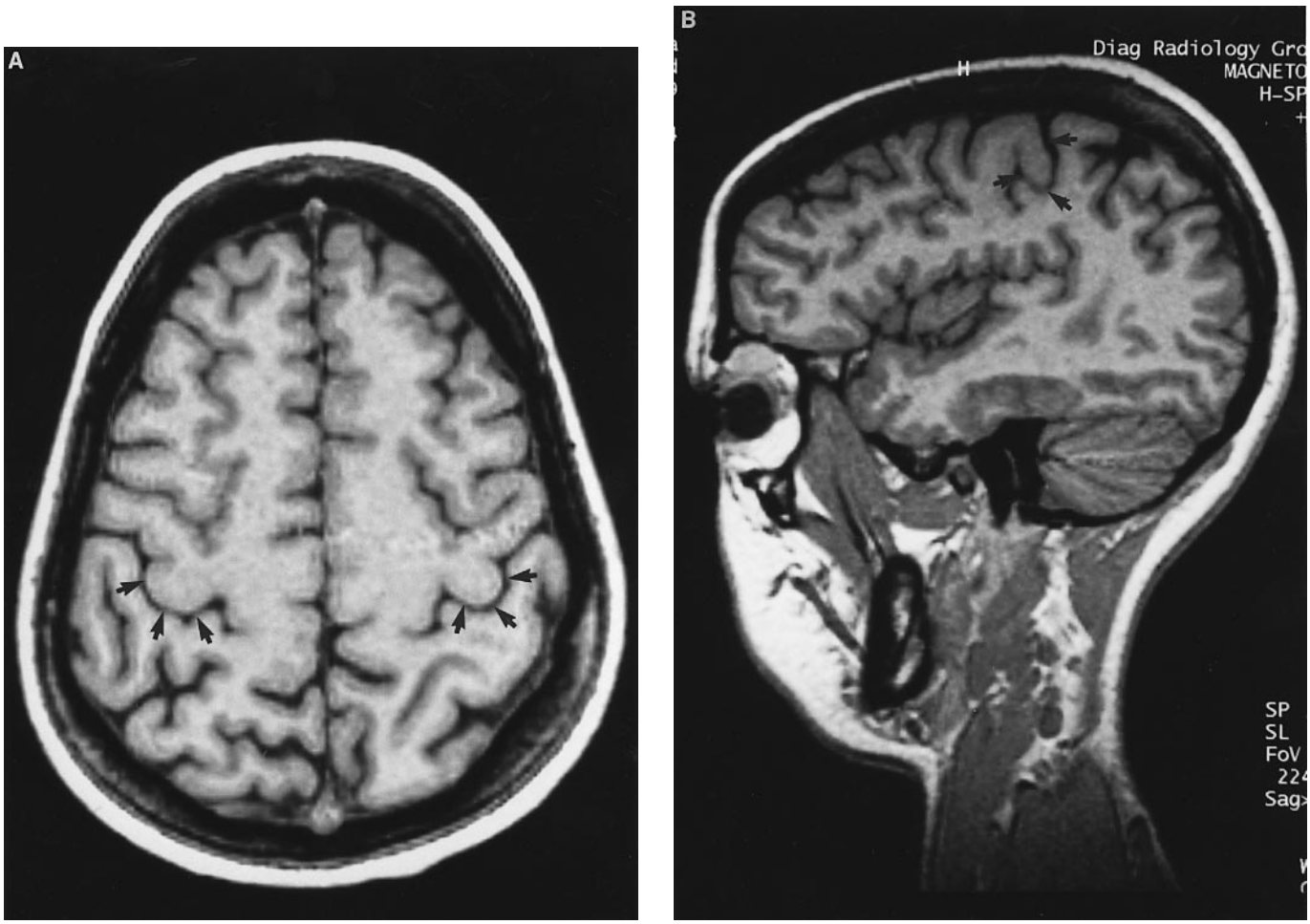

Fig. 8 An MPRAGE sequence in a volunteer. Axially (**A**) the precentral knob is omega-shaped in the left and epsilon-shaped in the right hemisphere. The knobs are posterior to the intersection of the superior frontal sulcus with the precentral sulcus. Sagittally (**B**) the posteriorly directed hook is identified at the level of the posterior part of the insula.

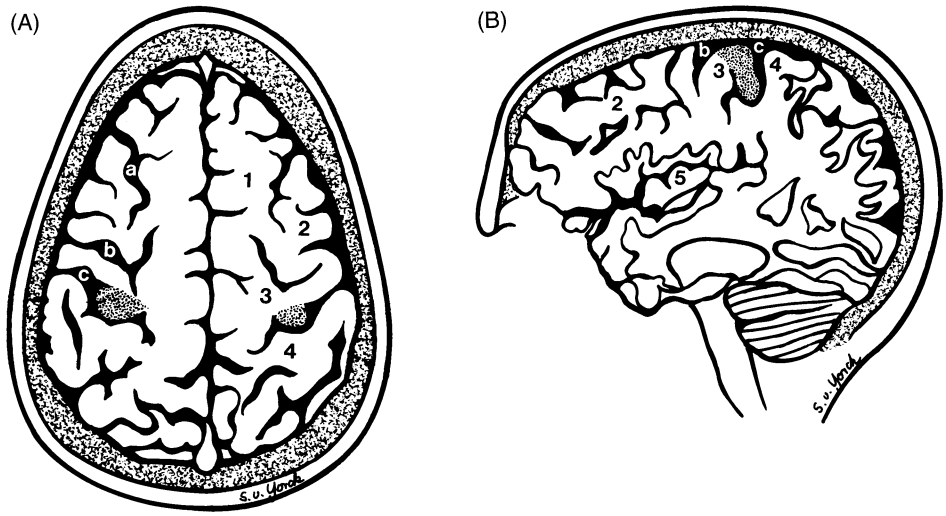

Fig. 9 Schematic drawing of the precentral knob (shaded area) in the axial plane (**A**) and in the sagittal plane (**B**). The knob is a protrusion of the precentral gyrus (3) into the central sulcus (c). It is located posterior to the intersection of the superior frontal sulcus (a) that divides the superior (1) from the middle (2) frontal gyrus, and the precentral sulcus (b). In the sagittal plane, at the level of the posterior part of the insula (5), the knob has the shape of a posteriorly directed hook facing the postcentral gyrus (4).

Table 3 *Evaluation of methods to define the precentral gyrus*

Score	Knob axial (Ω, ε)		Lateral axial		Knob sagittal (hook)		Lateral sagittal	
	Unaffected	Affected	Unaffected	Affected	Unaffected	Affected	Unaffected	Affected
n(score 0)	0	2	0	2	5	2	1	0
n(score 1)	3	0	4	4	5	1	6	4
n(score 2)	56	39	55	35	49	38	52	37
Total ($N = \Sigma n$)*	59	41	59	41	59	41	59	41
Mean score†	1.9	1.9	1.9	1.8	1.7	1.9	1.9	1.9
Detection rate (%)‡	100	95	100	95	92	95	98	100
P value; *t* test	$P \leqslant 0.005$§	n.s.	$P \leqslant 0.025$§	n.s.	n.s.	n.s.	n.s.	n.s.

Scores: 0 = structure not present; 1 = structure most probably present; 2 = structure present. *N = number of hemispheres evaluated with MPRAGE sequence: of the total 100 hemispheres, 59 were unaffected by a pathology [*see* (4) and (5) in Table 1B] and 41 were affected by a pathology [*see* (7) in Table 1B]. †Mean score = $[2\times n(\text{score } 2)+n(\text{score1})]/N$. ‡Detection rate is the percentage of hemispheres where the knob was either 'present' (score 2) or 'most probably present' (score 1). §Significant difference from the knob sagittal method; n.s. = no statistically significant differences from findings obtained with any of the other techniques.

and they may also contribute to postcentral gyrus activation (Goldberg, 1985).

Interestingly, these areas of postcentral activation, whether motor or sensory, are located just opposite to the precentral knob, the common location of the motor hand area. This close vicinity of cortical representation of motor and probably also sensory hand function which we found using fMRI is in line with Penfield and Boldrey's (1937) description of partially overlapping 'homunculi' of cortical sensory and motor representation. These findings were later confirmed when the cortical topography of hand motor representation (assessed using direct cortical stimulation) was compared with the topographical distribution of somatosensory evoked potentials (recorded with surface and depth electrodes from the surface of the sensorimotor cortex) following electrical nerve stimulation at the wrist (Jasper *et al*., 1960; Stohr and Goldring, 1969; Broughton *et al*., 1981; Allison *et al*., 1989) or following mechanical tapping of the skin of the fingers and hand (Woolsey *et al*., 1979).

Finally, it was interesting to compare the location of the motor hand area as determined by fMRI with the stimulation results of Penfield and Boldrey (1937) who pooled the results of 126 operations obtained with intrasurgical cortical stimulation. Penfield and Boldrey (1937) defined 'hand movement' as a movement in the metacarpo-phalangeal joints only, they looked at single or grouped finger movements separately, and they displayed the stimulation results for hand movement only in combination with the results for arm and shoulder movement. In this way they found that 'the responsive points extend 5.5 cm along the length of the fissure of Rolando', with a 'curious subgrouping of responses 1–2 cm in front of the central fissure'. In variance to their study (Penfield and Boldrey, 1937), our paradigm was 'opening and closure of the hand' that included a combination of metacarpophalangeal and finger movement and explicitly excluded more proximal movements of the upper limb. For such differences of the movement paradigms, the data of Penfield and Boldrey (1937) cannot be directly compared with our data. However, the MRI and anatomical sections presented in our study reveal that the part of the precentral gyrus opposite to the middle genu of the central sulcus, where Penfield and Boldreys' (1937) figures show a concentration of finger and upper limb motor sites, corresponds exactly to the precentral knob, where we found motor hand (metacarpophalangeal and finger) function to be represented using fMRI.

Detailed anatomy of the motor hand area

In a study concerning the anatomical localization of tumours, Salamon *et al.* (1991) describe the 'presence of a typical hook corresponding to the hand area projection' with 'a true and clearly insulization of that area' (Salamon *et al*., 1991). Talairach and Tournoux (1993) also describe this structure when viewed in the sagittal plane as being 'bayonet-shaped', 'step-like' or a 'zigzag'. From these descriptions, these authors are unquestionably referring to what we term the precentral knob, which appears hook-like when viewed in the sagittal plane. Only recently, this knob was also described as a 'knuckle' (Naidich and Brightbill, 1995) and as an 'Ω-shaped structure' (Puce *et al*., 1995) when viewed in the axial plane.

Classically, the central sulcus is divided into genua, a term first used by Broca (cited by Testut, 1911). Whereas Broca as well as Dejerine (1895) define two genua (superior and inferior, both anteriorly convex), Testut (1911) describes three (superior, middle and inferior genu, the middle being posteriorly convex, in contrast to the other two that are anteriorly convex). Cunningham (1892) as well as Ono *et al.* (1990) define two genua, but they describe the superior one as being posteriorly convex, probably consisting of both the superior and middle genu of Testut (1911), disregarding the first because of its smallness. Talairach and Tournoux (1993) refer to the shape of the central sulcus as a 'lengthened italic S', without using the term genua. In other reports the

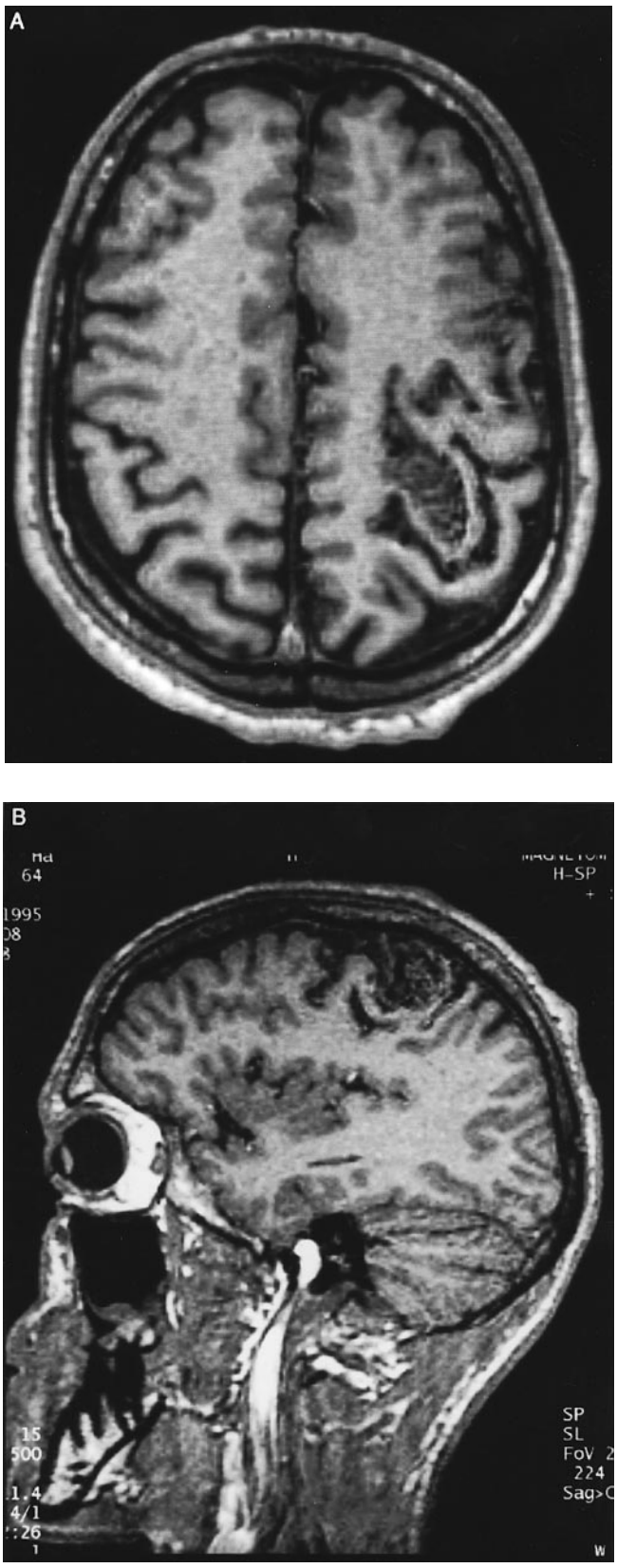

Fig. 10 An MPRAGE sequence of a patient with a precentrally located AVM. In the axial plane (**A**) the precentral knob is widely enlarged by the AVM, yet it can still be recognized and identified. In the sagittal plane (**B**), the AVM projects onto the tip of the hook, depressing it anteriorly and inferiorly.

precentral gyrus is divided into an upper, middle and lower third (Eberstaller, 1890).

All of these descriptions are qualitative providing no anatomical or morphometric criteria for defining limits or boundaries of these divisions. In contrast, the precentral knob we described in this report is a specifically defined segment of the precentral gyrus. The knob projects to the middle genu of the central sulcus (the base of its apex) (Figs 4 and 5). This knob could be regarded either as an 'insulization' (Salamon *et al*., 1991) or as a protrusion of the precentral gyrus towards the central sulcus. It is created by two anteriorly directed fissures that, as they deepen toward the base of the knob, give it its characteristic inverted omega shape (90% of hemispheres). Occasionally a third fissure courses between these two fissures, changing the knob's appearance from that of an inverted omega to a horizontal epsilon (10% of hemispheres). When changing the observation plane from the axial to the sagittal plane, the appearance of the knob changes to the shape of a posteriorly directed hook.

In five of the 59 hemispheres without a space-occupying lesion in our study (Table 1, step II), the knob could not be identified on images obtained in the sagittal plane even with optimal imaging techniques (MPRAGE). In these cases, variations in the course of one of the fissures were primarily responsible for altering appearance of the knob. This in turn resulted in a lower detection rate in the sagittal plane (92%) compared with the axial plane (100%) (Table 4).

It was occasionally difficult to identify the motor hand area by its hook appearance on sagittal sections of conventional slice thickness (5 mm), because the sections were too thick to allow good resolution of this small structure. This difficulty was reflected in the lower detection rate with which the hook was identified (79–88%) on the conventional images as compared with MPRAGE sequences in this study (92–95%).

The motor hand area during surgery

As outlined in Figs 4 and 5, the configuration of the middle genu of the central sulcus is less characteristic at the cortical surface than it is at deeper levels where it appears as the precentral knob. An additional problem in locating this genu early during surgery is that the arachnoid membrane and bridging veins obscure this structure. However, the precentral knob can be identified intraoperatively with ease as the structure opposite to the intersection of the superior frontal with the precentral sulcus. This enables the neurosurgeon to locate the motor hand area simply by inspecting the cortical surface.

A new method to locate the precentral gyrus

Several methods have become established to identify the precentral gyrus using various landmarks. These are superficial cortical, identifying (i) the superior frontal and precentral sulcus (Kido *et al*., 1980), (ii) the anterior ascending

Table 4A *Reliability of knob detection by three observers (readers T.A.Y., U.D.S., A.P.) using the axial knob method (Ω, ε)*

Score	Reader A				Reader B				Reader C				Consensus of all readers			
	Unaff		Aff		Unaff		Aff		Unaff		Aff		Unaff		Aff	
	MPR	Other	MPR	Other	MPR	Other	MPR	Other	MPR	Other	MPR	Other	MPR	Other	MPR	Other
n(score 0)	0	0	2	2	2	1	2	3	1	0	2	2	0	0	2	2
n(score 1)	3	0	0	2	5	1	1	2	4	0	0	3	–	–	–	–
n(score 2)	56	40	39	54	52	38	38	53	54	40	39	53	59	40	39	56
Total ($N = \Sigma n$)	59	40	41	58	59	40	41	58	59	40	41	58	59	40	41	58
Mean score	1.9	2.0	1.9	1.9	1.8	1.9	1.9	1.9	1.9	2.0	1.9	1.9	–	–	–	–
Detection rate (%)	–	–	–	–	–	–	–	–	–	–	–	–	100	100	95	97
Correct positive (*n*)	59	40	39	56	57	39	39	55	58	40	38	56	–	–	–	–
Correct negative (*n*)	0	0	2	2	0	0	2	2	0	0	2	2	–	–	–	–
False positive (*n*)	0	0	0	0	0	0	0	0	0	0	1	0	–	–	–	–
False negative (*n*)	0	0	0	0	2	1	0	1	1	0	0	0	–	–	–	–
Accuracy (%)	100	100	100	100	97	98	100	98	98	100	98	100	–	–	–	–
Sensitivity (%)	100	100	100	100	97	98	100	98	98	100	100	100	–	–	–	–

Scores: 0 = structure not present; 1 = structure most probably present; 2 = structure present. Consensus = consensus of all readers was obtained with the use of all methods to define the central sulcus (all cases, $n = 200$ hemispheres) and with the aid of a software program (MPRAGE, $n = 100$ hemispheres, Table 1). In this consensus discussion, it was only stated whether a knob was 'present' or 'not present'. This discussion took place after each of the readers had made his individual and written statement. Unaff = unaffected: both hemispheres of healthy subjects and non-affected hemispheres of patients were tested, either with MPRAGE [*see* (4) and (5) in Table 1B] or with other techniques [*see* (6) in Table 1B]. Aff = affected: hemispheres of patients, tested either with MPRAGE [*see* (7) in Table 1B] or with other techniques [*see* (6) in Table 1B]. Detection rate = percentage of hemispheres where the knob was either 'present' (score = 2) or 'most probably present' (score = 1). Correct positive = correct identification of knobs by an individual reader according to the consensus of all readers. Correct negative = correct 'failure to identify the knob' by an individual reader according to the consensus of all readers. False positive = erronous identification of a structure as the knob by an individual reader according to the consensus. False negative = failure to detect the knob by an individual reader according to the consensus. Accuracy = number of correct positive and correct negative identifications divided by the total number of hemispheres examined. Sensitivity = number of correct positive identifications divided by the sum of correct positive and false negative identifications.

Table 4B *Reliability of knob detection by three observers (readers T.A.Y., U.D.S., A.P.) using the sagittal knob method (hook)*

Score	Reader A				Reader B				Reader C				Consensus of all readers			
	Unaff		Aff		Unaff		Aff		Unaff		Aff		Unaff		Aff	
	MPR	Other	MPR	Other	MPR	Other	MPR	Other	MPR	Other	MPR	Other	MPR	Other	MPR	Other
n(score 0)	5	1	2	1	7	1	2	3	5	2	2	1	5	1	2	3
n(score 1)	5	2	1	5	6	2	0	4	5	2	0	4	–	–	–	–
n(score 2)	49	5	38	8	46	5	39	7	49	4	39	9	54	7	39	11
Total ($N = \Sigma n$)	59	8	41	14	59	8	41	14	59	8	41	14	59	8	41	14
Mean score	1.7	1.5	1.9	1.5	1.7	1.5	1.9	1.3	1.7	1.3	1.9	1.6	–	–	–	–
Detection rate (%)	–	–	–	–	–	–	–	–	–	–	–	–	92	88	95	79
Correct positive (*n*)	54	7	39	11	52	6	39	11	53	6	38	11	–	–	–	–
Correct negative (*n*)	5	1	2	1	5	1	2	3	5	1	2	1	–	–	–	–
False positive (*n*)	0	0	0	2	0	1	0	0	0	0	0	2	–	–	–	–
False negative (*n*)	0	0	0	0	2	0	0	0	1	1	1	0	–	–	–	–
Accuracy (%)	100	100	100	86	97	88	100	100	98	88	98	86	–	–	–	–
Sensitivity (%)	100	100	100	100	96	100	100	100	98	86	97	100	–	–	–	–

For explanations *see* footnotes of Table 4A.

and horizontal rami of the sylvian fissure (Ebeling *et al*., 1989; Naidich *et al*., 1995) and (iii) the ramus marginalis of the cingulate sulcus (Naidich and Brightbill, 1996), or deep cerebral as the anterior and posterior commissure (Talairach and Tournoux, 1988). It has been demonstrated that interindividual variability of these landmarks (Steinmetz *et al*., 1990) and intermethod or interrater discordances make these methods of identifying the precentral gyrus unreliable in 33–50% of cases (Sobel *et al*., 1993). More stable landmarks could be of value in increasing the accuracy with which the precentral gyrus is identified.

The precentral knob we describe is just such a landmark.

In the axial plane it was present in 100% of unaffected hemispheres (Table 4A) and in 96% of hemispheres affected by a wide spectrum of pathologies (Table 1). In the sagittal plane, the knob could be recognized as a typical hook in 91% of affected and unaffected hemispheres (Table 4B). The precentral knob is therefore a stable and eyecatching landmark, which is also reflected in its early, and mostly uncommented, description in atlases of the brain (Dejerine, 1895; Salamon *et al*., 1990; Duvernois, 1991; Kretschmann and Weinrich, 1991; Truwit and Lempert, 1994; Damasio, 1995).

The superior frontal sulcus, on the other hand, has been found to follow its 'classic' continuous course in only 40% of right and 32% of left hemispheres, and the expected connection between this sulcus and the precentral sulcus was lacking in 8% of the right hemispheres studied (Ono *et al*., 1990). The use of this sulcus as a landmark is further complicated by the presence of a doubled precentral sulcus (4% of cases) or a connection between the precentral and the central sulcus (12% of right hemispheres and 28% of left hemispheres) (Ono *et al*., 1990). We assume that these variations are the main reason for the report of large interrater variability in identifying these landmarks (Sobel *et al*., 1993).

In contrast to these results using other methods to locate the precentral gyrus, our method, using the precentral knob, provides consistent results as shown by high interrater agreement, even when assessed by comparatively unexperienced readers (Table 4A and B).

Suggested procedure to identify the precentral gyrus

We suggest that, in the axial plane, for its simplicity, the precentral knob should be identified first. The result should then be confirmed through the identification of the typical connection of the superior frontal with the precentral sulcus, and possibly through definition of the marginal ramus of the cingulate sulcus that reaches the midline cortical surface just behind the central sulcus. In the sagittal plane, because of its slight superiority, we would prefer to begin with the lateral sagittal method (Naidich *et al*., 1995), and incorporate the identification of the hook as one additional step in that system to help confirm the results. It is obvious that no method exists that could replace the detailed knowledge of the complex anatomy of the cortical surface, but we hope to have described a method that will ease the identification process.

Acknowledgements

We thank Diana Mathis, a professional communications consultant, for editing the manuscript. Financial support for this study came from the Friedrich Baur Foundation, Munich (to T.A.Y. and U.D.S.), the Weigand Foundation, Munich (to T.A.Y.), the Münchner Medizinische Wochenschrift (to T.A.Y.) and the Swiss National Science Foundation (Grant No. 32–9001.86, to U.D.S.).

References

Allison T, McCarthy G, Wood CC, Darcey TM, Spencer DD, Williamson PD. Human cortical potentials evoked by stimulation of the median nerve. II. Cytoarchitectonic areas generating short-latency activity. J Neurophysiol 1989; 62: 694–710.

Atlas SW, Howard RS, Maldjian J, Alsop D, Detre JA, Listerud J, et al. Functional magnetic resonance imaging of regional brain activity in patients with intracerebral gliomas: findings and implications for clinical management. Neurosurgery 1996; 38: 329–38.

Brodmann K. Vergleichende Lokalisationslehre der Grosshirnrinde. Leipzig: J.A. Barth, 1909.

Broughton R, Rasmussen T, Branch C. Scalp and direct cortical recordings of somatosensory evoked potentials in man (circa 1967). Can J Psychol 1981; 35: 136–58.

Connelly A, Jackson GD, Frackowiak RS, Belliveau JW, Vargha-Khadem F, Gadian DG. Functional mapping of activated human primary cortex with a clinical MR imaging system. Radiology 1993; 188: 125–30.

Constable RT, McCarthy G, Allison T, Anderson AW, Gore JC. Functional brain imaging at 1.5 T using conventional gradient echo MR imaging techniques. Magn Reson Imaging 1993; 11: 451–9.

Cunningham D. Contribution to the surface anatomy of the cerebral hemispheres. Dublin: Hodges, Figgis and Co., 1892.

Damasio H. Human brain anatomy in computerized images. New York: Oxford University Press, 1995.

Dejerine J. Anatomie des centres nerveux. Paris: Rueff et Cie, 1895.

Duvernoy HM. The human brain. Wien: Springer, 1991.

Ebeling U, Steinmetz H, Huang YX, Kahn T. Topography and identification of the inferior precentral sulcus in MR imaging. AJR Am J Roentgenol 1989; 153: 1051–6.

Eberstaller O. Ein Beitrag zur Anatomie der Oberfläche des Grosshirns. Wien: Urban and Schwarzenberg, 1890.

Foerster O. The motor cortex in man in the light of Hughlings Jackson's doctrines. Brain 1936; 59: 135–59.

Frahm J, Merboldt KD, Hanicke W. Functional MRI of human brain activation at high spatial resolution. Magn Reson Med 1993; 29: 139–44.

Goldberg G. Supplementory motor area strucure and function. Review and hypotheses. Behav Brain Sci 1985; 8: 567–615.

Jack CR Jr, Thompson RM, Butts RK, Sharbrough FW, Kelly PJ, Hanson DP, et al. Sensory motor cortex: correlation of presurgical mapping with functional MR imaging and invasive cortical mapping. Radiology 1994; 190: 85–92.

Jasper H, Lende R, Rasmussen T. Evoked potentials from the exposed somato-sensory cortex in man. J Nerv Ment Dis 1960; 130: 526–37.

Kahn T, Schwabe B, Bettag M, Harth T, Ulrich F, Rassek M, et al. Mapping of the cortical motor hand area with functional MR imaging and MR imaging—guided laser-induced interstitial thermotherapy of brain tumors. Radiology 1996; 200: 149–57.

Kido DK, LeMay M, Levinson AW, Benson WE. Computed tomographic localization of the precentral gyrus. Radiology 1980; 135: 373–7.

Kim SG, Ashe J, Georgopoulos AP, Merkle H, Ellermann JM, Menon RS, et al. Functional imaging of human motor cortex at high magnetic field. J Neurophysiol 1993a; 69: 297–302.

Kim SG, Ashe J, Hendrich K, Ellermann JM, Merkle H, Ugurbil K, et al. Functional magnetic resonance imaging of motor cortex: hemispheric asymmetry and handedness. Science 1993b; 261: 615–7.

Kretschmann H, Weinrich W. Klinische Neuroanatomie und kranielle Bilddiagnostik: Computertomographie und Magnetresonanztomographie. Stuttgart: Thieme, 1991.

Kwong KK, Belliveau JW, Chesler DA, Goldberg IE, Weisskoff RM, Poncelet BP, et al. Dynamic magnetic resonance imaging of human brain activity during primary sensory stimulation. Proc Natl Acad Sci U S A 1992; 89: 5675–9.

Lai S, Hopkins AL, Haacke EM, Li D, Wasserman BA, Buckley P, et al. Identification of vascular structures as a major source of signal contrast in high resolution 2D and 3D functional activation imaging of the motor cortex at 1.5T: preliminary results. Magn Reson Med 1993; 30: 387–92.

Menon RS, Ogawa S, Tank DW, Ugurbil K. Tesla gradient recalled echo characteristics of photic stimulation-induced signal changes in the human primary visual cortex. Magn Reson Med 1993; 30: 380–6.

Naidich TP, Brightbill T. The intraparietal sulcus: a landmark for localization of pathology on axial CT scans. Int J Neuroradiol 1995; 1: 3–16.

Naidich TP, Brightbill TC. The pars marginalis: Part I: a 'bracket' sign for the central sulcus in axial plane CT and MRI. Int J Neuroradiol 1996; 2: 3–19.

Naidich TP, Valavanis AG, Kubik S. Anatomic relationships along the low-middle convexity: Part I--Normal specimens and magnetic resonance imaging. Neurosurgery 1995; 36: 517–32.

Nii Y, Uematsu S, Lesser RP, Gordon B. Does the central sulcus divide motor and sensory functions? Cortical mapping of human hand areas as revealed by electrical stimulation through subdural grid electrodes. Neurology 1996; 46: 360–7.

Ogawa S, Tank DW, Menon R, Ellermann JM, Kim SG, Merkle H, et al. Intrinsic signal changes accompanying sensory stimulation: functional brain mapping with magnetic resonance imaging. Proc Natl Acad Sci U S A 1992; 89: 5951–5.

Ono M, Kubik S, Abernathey CD. Atlas of the cerebral sulci. Stuttgart: Thieme, 1990.

Penfield W, Boldrey E. Somatic motor and sensory representation in the cerebral cortex of man as studied by electrical stimulation. Brain 1937; 60: 389–443.

Penfield W, Rasmussen T. The cerebral cortex of man. New York: Macmillan, 1950.

Puce A, Constable RT, Luby ML, McCarthy G, Nobre AC, Spencer DD, et al. Functional magnetic resonance imaging of sensory and motor cortex: comparison with electrophysiological localization. J Neurosurg 1995; 83: 262–70.

Rao SM, Binder JR, Bandettini PA, Hammeke TA, Yetkin FZ, Jesmanowicz A, et al. Functional magnetic resonance imaging of complex human movements. Neurology 1993; 43: 2311–8.

Rao SM, Binder JR, Hammeke TA, Bandettini PA, Bobholz JA, Frost JA, et al. Somatotopic mapping of the human primary motor cortex with functional magnetic resonance imaging. Neurology 1995; 45: 919–24.

Rumeau C, Tzourio N, Murayama N, Peretti-Viton P, Levrier O, Joliot M, et al. Location of hand function in the sensorimotor cortex: MR and functional correlation. AJNR Am J Neuroradiol 1994; 15: 567–72.

Salamon G, Raynaud C, Regis J, Rumeau C. Magnetic resonance imaging of the pediatric brain: an anatomical atlas. New York: Raven Press, 1990.

Salamon G, Martini P, Ternier F, Vibert E, Murayama N, Khadr E. Topographical study of supratentorial brain tumors. [Review]. J Neuroradiol 1991; 18: 123–40.

Schad LR, Trost U, Knopp MV, Muller E, Lorenz WJ. Motor cortex stimulation measured by magnetic resonance imaging on a standard 1.5 T clinical scanner. Magn Reson Imaging 1993; 11: 461–4.

Sobel DF, Gallen CC, Schwartz BJ, Waltz TA, Copeland B, Yamada S, et al. Locating the central sulcus: comparison of MR anatomic and magnetoencephalographic functional methods [see comments]. AJNR Am J Neuroradiol 1993; 14: 915–25. Comment in: AJNR Am J Neuroradiol 1993; 14: 926–7.

Steinmetz H, Furst G, Freund HJ. Variation of perisylvian and calcarine anatomic landmarks within stereotaxic proportional coordinates. AJNR Am J Neuroradiol 1990; 11: 1123–30.

Stohr PE, Goldring S. Origin of somatosensory evoked scalp responses in man. J Neurosurg 1969; 31: 117–27.

Talairach J, Tournoux P. Co-planar stereotaxic atlas of the human brain: 3-dimensional proportional system: An approach to cerebral imaging. Stuttgart: Thieme, 1988.

Talairach J, Tournoux P. Referentially oriented cerebral MRI anatomy. Stuttgart, New York: Thieme, 1993.

Testut L. Traite d'anatomie humaine. Paris: Octave Doin et Fils, 1911.

Truwit CL, Lempert TE. High resolution atlas of cranial neuroanatomy. Baltimore: Williams and Wilkins, 1994.

Turner R, Jezzard P, Wen H, Kwong KK, Le Bihan D, Zeffiro T, et al. Functional mapping of the human visual cortex at 4 and 1.5 tesla using deoxygenation contrast EPI. Magn Reson Med 1993; 29: 277–9.

Uematsu S, Lesser R, Fisher RS, Gordon B, Hara K, Krauss GL, et al. Motor and sensory cortex in humans: topography studied with chronic subdural stimulation [see comments]. Neurosurgery 1992a; 31: 59–71. Comment in: Neurosurgery 1993; 33: 340–1.

Uematsu S, Lesser RP, Gordon B. Localization of sensorimotor cortex: the influence of Sherrington and Cushing on the modern concept. Neurosurgery 1992b; 30: 904–12.

Werner J. Medizinische Statistik. München: Urban & Schwarzenberg, 1984.

Woolsey CN, Erickson TC, Gilson WE. Localization of somatic sensory and motor areas of human sensory cortex as determined by direct recording of evoked potentials and electrical stimulation. J Neurosurg 1979; 51: 476–506.

Yousry T, Schmidt D, Alkadhi H, Schmid UD, Winkler PA, Peraud A. The precentral knob: a characteristic anatomical structure representing the motor hand area [abstract]. Neuroradiology 1995a; 37 Suppl 1: S 49.

Yousry TA, Schmid UD, Jassoy AG, Schmidt D, Eisner WE, Reulen HJ, et al. Topography of the cortical motor hand area: prospective study with functional MR imaging and direct motor mapping at surgery. Radiology 1995b; 195: 23–9.

Yousry TA, Schmid UD, Schmidt D, Hagen T, Jassoy A, Reiser MF. The central sulcal vein: a landmark identifying the central sulcus by functional MRI. J Neurosurg 1996; 85: 608–17.

Received May 17, 1996. Revised July 31, 1996.
Accepted August 23, 1996